

Condensation of Classical Nonlinear Waves in a Two-Component System

Hayder Salman and Natalia G. Berloff

Department of Applied Mathematics and Theoretical Physics, University of Cambridge, Cambridge, CB3 0WA, UK

Abstract

We study the formation of large-scale coherent structures (condensates) for a system of two weakly interacting Bose gases in the semiclassical approximation. Using the coupled defocusing nonlinear Schrödinger (NLS) equations as a representative model, we focus on condensation in the phase mixing regime. We employ weak turbulence theory to provide a complete thermodynamic description of the classical condensation process. We show that the temperature and the condensate mass fractions are fully determined by the total number of particles in each component and the initial total energy. Moreover, we find that, at higher energies, condensation can occur in only one component. We derive an analytic result for the variation of the critical energy where this transition occurs. The theory presented provides excellent agreement with results of numerical simulations obtained by directly integrating the dynamical model.

Key words: Bose-Einstein condensates, Weak turbulence theory, Nonlinear Schrödinger equations

PACS: 03.65.Sq, 03.75.Kk, 05.65.+b, 42.65.Sf

1. Introduction

Many classical systems in nature reveal the emergence of large scale coherent structures from a background irregular field characterised by small-scale fluctuations. Examples of systems that exhibit such behaviour include classical turbulence, nonlinear optics, superfluids, ultracold gases and Bose-Einstein Condensates (BECs), and the formation of the early universe. In certain regions of the parameter space, a large sub-class of these systems can be described by a system of weakly nonlinear dispersive waves. A universal equation that governs the evolving field in such scenarios is then given by the Nonlinear Schrödinger (NLS) equation. The process of self-organisation in the focusing NLS equation has been studied in [1]. It was found that a large-scale solitary wave tends to emerge from a sea of small-scale turbulent fluctuations. In this work, we concentrate on the defocusing NLS equations. This equation has been receiving increasing attention due to the experimental advances in BECs. In this context, the defocusing NLS equation corresponds to the Gross-Pitaevskii (GP) equation [2] of a homogeneous Bose gas. The GP equation has long been used as a model of a weakly interacting Bose gas at zero temperature. More recently, it has been argued [3] that the GP equation can be used to model the long wavelength part of the spectrum of a BEC at finite temperatures. Numerical simulations conducted within this framework [4], [5] have

indeed confirmed this, revealing the ability of the model to capture the formation of a condensate from an initially turbulent state.

With the rapid developments being made in experimental techniques, it is now possible to realize multi-component BECs formed by the simultaneous trapping and cooling of atoms in distinct spin or hyperfine levels [6] or different atomic species [7]. The finite temperature dynamics of such Bose gas mixtures is then governed by a system of coupled NLS equations. An important question that subsequently arises is “*How can we describe the thermodynamic state of such a two-component system?*” This would then allow a clear specification of the temperature of the system which in turn would provide a means to quantify effects such as the mutual friction between the thermal cloud and superfluid vortices (see e.g. [8] for work addressing these aspects for a one-component Bose gas). Furthermore, whilst such two-component Bose gas mixtures are of interest in their own right, they also serve as idealised models to study symmetry-breaking phase transitions that are believed to have occurred in the early evolution of the universe. A specific example is given by the Kibble-Zurek mechanism [9] of the formation of topological defects following the rapid quench of the system below the point of second-order phase transitions. This scenario would correspond to the formation of cosmological *vortons* and *springs* that are analogous to the vortex ring-slaved wave and vortex ring-vortex ring

complexes of BECs [10]. In addition to these physical examples, the coupled NLS equations are also encountered in the study of optical fibres and electromagnetic waves [11]. Given the universality of these equations in the nonlinear sciences, an accurate thermodynamic description of the condensation process in such a system could have significant implications in various branches of physics.

In this paper, we will generalise the results presented in [12], that describe the condensation process of a one-component system, to a two-component system. We note that two-component systems tend to show a broad class of qualitatively different behavior depending on the relative strengths of the intercomponent and intracomponent interactions. This can lead to contrasting regimes of condensation: the phase mixing regime and the phase separation regime [13]. Consistent with the assumptions commonly used in weak turbulence theory, we will focus exclusively on the phase mixing regime.

2. Kinetic theory for two-component system

We begin by considering the scenario of a system of two weakly interacting Bose gases within the semiclassical approximation that have been rapidly cooled below the transition temperature. Their evolution from the resulting strongly nonequilibrium initial state is then described by the coupled NLS equations given by

$$\begin{aligned} i\partial_t\psi_1 &= -\nabla^2\psi_1 + |\psi_1|^2\psi_1 + \alpha|\psi_2|^2\psi_1, \\ i\partial_t\psi_2 &= -\nabla^2\psi_2 + |\psi_2|^2\psi_2 + \alpha|\psi_1|^2\psi_2, \end{aligned} \quad (1)$$

where ψ_1 and ψ_2 are complex-valued classical fields corresponding to each component, and α is the intracomponent coupling constant. For the phase mixing regime, we require $0 < \alpha < 1$. The dynamics governed by the above equations will conserve the total mass (number of particles) given by $N_1 = \int |\psi_1|^2 d\mathbf{x}$ and $N_2 = \int |\psi_2|^2 d\mathbf{x}$. In addition, the total energy (Hamiltonian) of the coupled system

$$H = \int \left[\sum_{i=1}^2 \left\{ |\nabla\psi_i|^2 + \frac{1}{2}|\psi_i|^4 \right\} + \alpha|\psi_1|^2|\psi_2|^2 \right] dV. \quad (2)$$

will be conserved. Without loss of generality we shall assume that $N_2 \leq N_1$.

Despite the formal reversibility of the above Hamiltonian system, the evolution of the nonlinear waves ψ_1 and ψ_2 is nonintegrable giving rise to an effective diffusion in phase space. This results in an *irreversible* evolution to thermal equilibrium. By invoking the random phase approximation (assumption of quasi-Gaussian statistics), it is possible to derive closed irreversible kinetic equations that describe the evolution of the system using Weak Turbulence Theory (WTT) [14]. For a homogeneous system, we accomplish this by expressing the order parameters in terms of their Fourier transforms $\psi_1 = \frac{1}{(2\pi)^{3/2}} \int a_{\mathbf{k}}(t) e^{i\mathbf{k}\cdot\mathbf{x}} d\mathbf{k}$, $\psi_2 = \frac{1}{(2\pi)^{3/2}} \int b_{\mathbf{k}}(t) e^{i\mathbf{k}\cdot\mathbf{x}} d\mathbf{k}$. Substituting into Eq. (2), we can derive expressions for the spectral number densities

$\langle a_{\mathbf{k}_1} a_{\mathbf{k}_2}^* \rangle = n_1 \delta(\mathbf{k}_1 - \mathbf{k}_2)$; $\langle b_{\mathbf{k}_1} b_{\mathbf{k}_2}^* \rangle = l_1 \delta(\mathbf{k}_1 - \mathbf{k}_2)$. Provided the nonlinearity in the system is sufficiently weak (i.e. $N_1/V \ll 1$; $N_2/V \ll 1$; $\alpha \ll 1$, where V is the volume of the system), we can derive the kinetic equations

$$\begin{aligned} \partial_t n_k &= \frac{4\pi}{(2\pi)^6} \int \left(\left[(n_k + n_1)n_2 n_3 - n_k n_1 (n_2 + n_3) \right] \right. \\ &\quad \left. + \alpha^2 \left[(n_k + l_1)l_2 n_3 - n_k l_1 (l_2 + n_3) \right] \right) \\ &\quad \times \delta(\mathbf{k} + \mathbf{k}_1 - \mathbf{k}_2 - \mathbf{k}_3) \delta(k^2 + k_1^2 - k_2^2 - k_3^2) d\mathbf{k}_1 d\mathbf{k}_2 d\mathbf{k}_3. \\ \partial_t l_k &= \frac{4\pi}{(2\pi)^6} \int \left(\left[(l_k + l_1)l_2 l_3 - l_k l_1 (l_2 + l_3) \right] \right. \\ &\quad \left. + \alpha^2 \left[(l_k + n_1)n_2 l_3 - l_k n_1 (n_2 + l_3) \right] \right) \\ &\quad \times \delta(\mathbf{k} + \mathbf{k}_1 - \mathbf{k}_2 - \mathbf{k}_3) \delta(k^2 + k_1^2 - k_2^2 - k_3^2) d\mathbf{k}_1 d\mathbf{k}_2 d\mathbf{k}_3. \end{aligned} \quad (3)$$

These equations conserve $N_1 = V \int n_{\mathbf{k}}(t) d\mathbf{k}$, $N_2 = V \int l_{\mathbf{k}}(t) d\mathbf{k}$, and the total kinetic energy $E = V \int k^2 (n_{\mathbf{k}}(t) + l_{\mathbf{k}}(t)) d\mathbf{k}$. They admit two formal equilibrium solutions; the first corresponding to a uniform distribution $n_{\mathbf{k}}^{\text{eq}} = c_1$, $l_{\mathbf{k}}^{\text{eq}} = c_2$, and the second given by the Rayleigh-Jeans (RJ) distribution

$$n_{\mathbf{k}}^{\text{eq}} = \frac{T}{k^2 - \mu_1}, \quad l_{\mathbf{k}}^{\text{eq}} = \frac{T}{k^2 - \mu_2}. \quad (4)$$

Here, T is the thermodynamic temperature, and μ_1 and μ_2 are the chemical potentials. Equation (3) satisfies a H-theorem for entropy growth which implies that the RJ distribution will be realized in practice. However, Eq. (4) provides only a formal solution since it leads to non-convergent expressions for N_1 , N_2 , and the kinetic energy E , as $k \rightarrow \infty$. We recall that, for BECs, Eq. (1) is valid in the limit of large occupation numbers where a semi-classical description is valid. When $n_{\mathbf{k}} \sim 1$ and $l_{\mathbf{k}} \sim 1$, Eq. (1) begins to break down and a full quantum mechanical treatment of the problem becomes necessary. To regularise the ultra-violet catastrophe, we introduce a cut-off k_c such that $n^{\text{eq}}(|k_c|) > 1$, $l^{\text{eq}}(|k_c|) > 1$. This cut-off does not affect the equilibrium state provided a sufficiently large number of modes can be represented classically [4,15]. The reason is that a full quantum mechanical description corresponds to a grand-canonical ensemble with fluctuations in particle number and energy. However, for sufficiently many modes, such fluctuations will be small and we can introduce the above truncation to reduce the system to a microcanonical ensemble where the number of particles and the energy are conserved. In practice, this cut-off is introduced by prescribing a particular grid resolution in our simulations. Such a cut-off can only guarantee that the above condition is satisfied at thermodynamic equilibrium but not necessarily throughout the transients (i.e. throughout the formation and growth of the condensates). Consequently, the nonequilibrium state of the system is generally grid-dependent whereas the thermodynamic state is well-defined. We will illustrate this point further below with our numerical simulations.

The RJ distribution corresponding to the solution of Eq. (3) is only valid at sufficiently high energies when no condensate is present. At sufficiently low energies, Eq. (3) breaks down very rapidly giving way to the formation of a condensate as elucidated in numerical simulations for a one-component system [4,5,12] and a two-component system [16]. In the simplest scenario, condensates with zero wavenumbers are formed and are associated with the uniform states provided we are in the phase mixing regime. If the condensates that form are strong in the sense that $(N_1 - n_o)/N_1 \ll 1$, $(N_2 - l_o)/N_2 \ll 1$ ($n_o = |a_o|^2$; $l_o = |b_o|^2$ are the occupation numbers of the condensates in components 1 and 2, respectively), one can describe the nonlinear dynamics at these later times by considering the evolution of small quasiparticle perturbations around the condensates. For our two-component system, we accomplish this by introducing the ansatz

$$a_k = [\sqrt{n_o}\delta(k) + \tilde{a}_k(t)]e^{-in_ot}, \quad (5)$$

$$b_k = [\sqrt{l_o}\delta(k) + \tilde{b}_k(t)]e^{-il_ot}. \quad (6)$$

Upon substituting these expressions into the Fourier-transform representation of Eq. (2), we introduce a transformation to diagonalise terms in the Hamiltonian that are quadratic in \tilde{a}_k and \tilde{b}_k . A generalisation of Bogoliubov's transformation [17] to diagonalise the Hamiltonian in two-component systems was given in [18]. To this end, we introduce the canonical variables $\mathcal{N} = (\xi_{\mathbf{k}}, \eta_{\mathbf{k}})^T$ which are related to the original variables $\mathcal{A} = (\tilde{a}_{\mathbf{k}}, \tilde{b}_{\mathbf{k}})^T$ through the relation

$$\begin{pmatrix} \mathcal{A} \\ \mathcal{A}^\dagger \end{pmatrix} = \begin{pmatrix} \mathcal{U}^+ & \mathcal{U}^- \\ \mathcal{U}^- & \mathcal{U}^+ \end{pmatrix} \begin{pmatrix} \mathcal{N} \\ \mathcal{N}^\dagger \end{pmatrix}, \quad (7)$$

where $\mathcal{N}^\dagger = (\xi_{-\mathbf{k}}^*, \eta_{-\mathbf{k}}^*)^T$, and $\mathcal{A} = (\tilde{a}_{-\mathbf{k}}^*, \tilde{b}_{-\mathbf{k}}^*)^T$. To preserve the properties of the Poisson bracket in the new basis, the transformation must satisfy the condition $\mathcal{U}^+ \mathcal{U}^{+T} - \mathcal{U}^- \mathcal{U}^{-T} = \mathbf{I}$. A transformation that satisfies this condition and diagonalises the quadratic term is obtained when the elements u_{ij}^\pm of the 2×2 transformation matrices \mathcal{U}^\pm are given by

$$\mathcal{U}^\pm = \begin{pmatrix} \frac{\Gamma_k^{+2} \pm 1}{2\Gamma_k^+} \cos \gamma_k & -\frac{\Gamma_k^{-2} \pm 1}{2\Gamma_k^-} \sin \gamma_k \\ \frac{\Gamma_k^{+2} \pm 1}{2\Gamma_k^+} \sin \gamma_k & \frac{\Gamma_k^{-2} \pm 1}{2\Gamma_k^-} \cos \gamma_k \end{pmatrix}. \quad (8)$$

$\Gamma_k^\pm = \sqrt{k^2/\Omega^\pm}$ denotes the ratios of the dispersion relations, where $\Omega^\pm = \sqrt{k^4 + c^\pm k^2}$ and

$$c^\pm = [n_o + l_o \pm \sqrt{(n_o - l_o)^2 + 4\alpha^2 n_o l_o}]/V, \quad (9)$$

$$\sin \gamma_k = \sqrt{\frac{1}{2} \left[1 - \frac{1-r}{\sqrt{(1-r)^2 + 4z^2}} \right]}, \quad (10)$$

$$\cos \gamma_k = \sqrt{\frac{1}{2} \left[1 + \frac{1-r}{\sqrt{(1-r)^2 + 4z^2}} \right]}, \quad (11)$$

where $r = l_o/n_o$ and $z = \alpha\sqrt{l_o/n_o}$. The resulting expression for the Hamiltonian leads to kinetic equations for the canonical (quasiparticle) densities $\langle \xi_{\mathbf{k}_1} \xi_{\mathbf{k}_2}^* \rangle = \tilde{n}_1 \delta(\mathbf{k}_1 - \mathbf{k}_2)$; $\langle \eta_{\mathbf{k}_1} \eta_{\mathbf{k}_2}^* \rangle = \tilde{l}_1 \delta(\mathbf{k}_1 - \mathbf{k}_2)$ which are given by

$$\begin{aligned} \partial_t \tilde{n}_k = \pi \int & \left([R_{k12} - R_{1k2} - R_{2k1}] + [S_{1k2} + S_{12k}] \right. \\ & \left. + [T_{k12} - T_{1k2}] + U_{k12} + V_{21k} \right) d\mathbf{k}_1 d\mathbf{k}_2, \end{aligned} \quad (12)$$

$$R_{k12} = \Delta_{k12}^{(1)} [\tilde{n}_1 \tilde{n}_2 - \tilde{n}_k \tilde{n}_1 - \tilde{n}_k \tilde{n}_2] \delta(\Omega_k^+ - \Omega_1^+ - \Omega_2^+),$$

$$S_{1k2} = \Delta_{1k2}^{(2)} [\tilde{n}_k \tilde{n}_2 - \tilde{l}_1 \tilde{n}_k - \tilde{l}_1 \tilde{n}_2] \delta(\Omega_1^- - \Omega_k^+ - \Omega_2^+),$$

$$T_{k12} = \Delta_{k12}^{(3)} [\tilde{n}_1 \tilde{l}_2 - \tilde{n}_k \tilde{n}_1 - \tilde{n}_k \tilde{l}_2] \delta(\Omega_k^+ - \Omega_1^+ - \Omega_2^-),$$

$$U_{k12} = \Delta_{k12}^{(4)} [\tilde{l}_1 \tilde{l}_2 - \tilde{n}_k \tilde{l}_1 - \tilde{n}_k \tilde{l}_2] \delta(\Omega_k^+ - \Omega_1^- - \Omega_2^-),$$

$$V_{21k} = \Delta_{21k}^{(5)} [\tilde{l}_1 \tilde{n}_k - \tilde{l}_2 \tilde{l}_1 - \tilde{l}_2 \tilde{n}_k] \delta(\Omega_2^- - \Omega_1^- - \Omega_k^+),$$

where $\Delta_{k12}^{(i)} = C_{k12}^{(i)} \delta(\mathbf{k} - \mathbf{k}_1 - \mathbf{k}_2)$ and $C^{(i)}$ denote coefficients that will, in general, depend on u_{ij}^\pm , n_o , l_o and α . Since we are only interested in equilibrium solutions, their precise form is not too important. The equation for \tilde{l}_k follows by symmetry of the dynamical equation. These kinetic equations are now given by resonant three-wave interactions and have a one parameter family of solutions given by

$$\tilde{n}_{\mathbf{k}}^{\text{eq}} = T/\Omega^+(k), \quad \tilde{l}_{\mathbf{k}}^{\text{eq}} = T/\Omega^-(k), \quad (13)$$

respectively. The condensates, therefore, strongly affect the equilibrium distributions of the quasiparticles.

We note that in contrast to the kinetic equations presented in [19] and [20] for the one-component case, Eq. (12) was derived assuming fixed amplitudes for the condensate densities n_o , and l_o as in [21]. The reader should be made aware that Eq. (12) and its counterpart for \tilde{l}_k are not applicable during the growth of the condensates. During such transient regimes, additional terms coupling the evolution of \tilde{n}_k and \tilde{l}_k to n_o and l_o would arise (see e.g. [20] for the one component system). However, at equilibrium, these terms vanish and, therefore, assuming n_o and l_o is justifiable for our purposes since we are specifically interested in thermodynamic states. Equation (12) can, therefore, be used to determine the equilibrium distribution functions of the quasiparticles at thermodynamic equilibrium.

3. Thermodynamic description

Using the equilibrium solutions of Eq. (12) stated above, we can now derive a relation between the occupation numbers n_o , l_o , and the total number of particles N_1 , N_2 and the energy H . For a finite sized system, the Hamiltonian can be expressed in terms of the Fourier series $\psi_1 = \frac{1}{\sqrt{V}} \sum_k a_k \exp(i\mathbf{k} \cdot \mathbf{x})$, $\psi_2 = \frac{1}{\sqrt{V}} \sum_k b_k \exp(i\mathbf{k} \cdot \mathbf{x})$. The Hamiltonian can then be written as $H = H_o + H_2 + H_3 + H_4$ depending on how $a_o = a_{k=0}$ and $b_o = b_{k=0}$, and non-zero modes enter the expansion:

$$\begin{aligned}
H_o &= \frac{1}{2V} [|a_o|^4 + |b_o|^4 + 2|a_o|^2(N_1 - |a_o|^2) \\
&\quad + 2|b_o|^2(N_2 - |b_o|^2)] + \frac{\alpha}{V} [|a_o|^2 N_2 + |b_o|^2 N_1], \\
H_2 &= \sum'_k [(k^2 + \frac{|a_o|^2}{V}) a_{\mathbf{k}} a_{\mathbf{k}}^* + \frac{1}{2V} (a_o^2 a_{\mathbf{k}}^* a_{-\mathbf{k}}^* + \text{c.c.})] \\
&\quad + \sum'_k [(k^2 + \frac{|b_o|^2}{V}) b_{\mathbf{k}} b_{\mathbf{k}}^* + \frac{1}{2V} (b_o^2 b_{\mathbf{k}}^* b_{-\mathbf{k}}^* + \text{c.c.})] \\
&\quad + \sum'_k [\frac{\alpha}{V} (a_o b_o a_{\mathbf{k}}^* b_{-\mathbf{k}}^* + a_o b_o^* a_{\mathbf{k}} b_{\mathbf{k}} + \text{c.c.})], \\
H_3 &= \sum_{k_1, k_2, k_3} [\frac{1}{2V} (2a_o a_{k_1} a_{k_2}^* a_{k_3}^* + 2b_o b_{k_1} b_{k_2}^* b_{k_3}^* + \text{c.c.}) \\
&\quad + \frac{\alpha}{V} (a_o b_{k_1} a_{k_2}^* b_{k_3}^* + b_o a_{k_1} a_{k_2}^* b_{k_3}^* + \text{c.c.})] \delta_{\mathbf{k}_1 - \mathbf{k}_2 - \mathbf{k}_3}, \\
H_4 &= \sum_{k_1, k_2, k_3, k_4} [\frac{1}{2V} (a_{k_1} a_{k_2} a_{k_3}^* a_{k_4}^* + b_{k_1} b_{k_2} b_{k_3}^* b_{k_4}^*) \\
&\quad + \frac{\alpha}{V} (a_{k_1} b_{k_2} a_{k_3}^* b_{k_4}^*)] \delta_{\mathbf{k}_1 + \mathbf{k}_2 - \mathbf{k}_3 - \mathbf{k}_4}. \tag{14}
\end{aligned}$$

In Eq. (14), \sum'_k denotes summation over k but excluding the $k = 0$ mode, and c.c. denotes the complex conjugate of the preceding terms. To relate the equilibrium distributions obtained from the kinetic equation (12) to this form of the Hamiltonian, we must diagonalise the quadratic term H_2 . Rewriting the Hamiltonian in terms of the basis $\mathcal{N} = (\xi_{\mathbf{k}}, \eta_{\mathbf{k}})^T$, the quadratic part takes the form $H_2 = \sum'_k (\Omega^+(k) \xi_k \xi_k^* + \Omega^-(k) \eta_k \eta_k^*)$. Now ensemble averaging the equations and using the equilibrium distributions $\tilde{n}_{\mathbf{k}}^{\text{eq}}$, and $\tilde{l}_{\mathbf{k}}^{\text{eq}}$ given above, we can express the occupation numbers of the two gases in the new basis as

$$N_1 - n_o = T \sum'_k \frac{(u_{11}^+ + u_{11}^-)}{\Omega^+(k)} + \frac{(u_{12}^+ + u_{12}^-)}{\Omega^-(k)}, \tag{15}$$

$$N_2 - l_o = T \sum'_k \frac{(u_{21}^+ + u_{21}^-)}{\Omega^+(k)} + \frac{(u_{22}^+ + u_{22}^-)}{\Omega^-(k)}. \tag{16}$$

We note that when $N_1 = N_2$, the two species have identical properties and Eqs. (15) and (16) must coincide. In this

case it can be shown, by setting $n_o = l_o$ in the expressions for c^\pm , $\sin \gamma_k$, and $\cos \gamma_k$ appearing in the transformation described above that this limit is correctly recovered by our equations.

The ensemble averaged Hamiltonian will have contributions from only H_o , H_2 , and H_4 . Rewriting the resulting expression in the new basis, we obtain

$$\begin{aligned}
\langle H \rangle &= E_0 + \sum'_k (\Omega_1(k) \tilde{n}_{\mathbf{k}}^{\text{eq}} + \Omega_2(k) \tilde{l}_{\mathbf{k}}^{\text{eq}}) \\
&= E_0 + 2T \sum'_k 1, \tag{17}
\end{aligned}$$

where

$$\begin{aligned}
E_0 &= \frac{1}{2V} [N_1^2 + (N_1 - n_o)^2 + N_2^2 + (N_2 - l_o)^2] \\
&\quad + \frac{\alpha}{V} [N_1 N_2], \tag{18}
\end{aligned}$$

denotes the energy of the ground state. Using either Eq. (15) or (16), we can eliminate the temperature in the expression for $\langle H \rangle$ to obtain

$$\begin{aligned}
\langle H \rangle &= E_0 + \frac{(N_1 - n_o) \sum'_k 1}{\sum'_k \left(\frac{(u_{11}^+ + u_{11}^-)}{\Omega^+(k)} + \frac{(u_{12}^+ + u_{12}^-)}{\Omega^-(k)} \right)}, \\
&= E_0 + \frac{(N_2 - l_o) \sum'_k 1}{\sum'_k \left(\frac{(u_{21}^+ + u_{21}^-)}{\Omega^+(k)} + \frac{(u_{22}^+ + u_{22}^-)}{\Omega^-(k)} \right)}. \tag{19}
\end{aligned}$$

This equation provides two algebraic relations for the two unknowns n_o and l_o given H , N_1 , N_2 .

At intermediate energies, we find that only one component condenses and the theory presented above breaks down (in practice resulting in negative values of l_o). In this part of the parameter space, we need to introduce the ansatz $a_k = [\sqrt{n_o} \delta(k) + \tilde{a}_k(t)] e^{-in_o t}$ only for the first component whilst assuming a purely continuous spectrum for the second component. This results in a coupled system of kinetic equations that are similar to Eqs. (3) and (12) above but where the first component is governed by three-wave resonances whereas the second is governed by four-wave resonances. These equations will have the equilibrium distributions $\tilde{n}_k = \frac{T}{\omega_B}$ and $\tilde{l}_k = \frac{T}{k^2 - \mu_2}$ where \tilde{n}_k is now defined as above but with l_o set to zero and $\omega_B = \sqrt{k^4 + 2n_o k^2/V}$ is the classical single-component Bogoliubov dispersion relation. Therefore, when only one component is condensed, we obtain the expressions

$$N_1 - n_o = T \sum'_k \frac{(k^2 + n_o/V)}{\omega_B^2(k)}, \tag{20}$$

$$N_2 = \sum_k \frac{T}{k^2 - \mu_2}. \tag{21}$$

The ensemble averaged Hamiltonian then takes the form

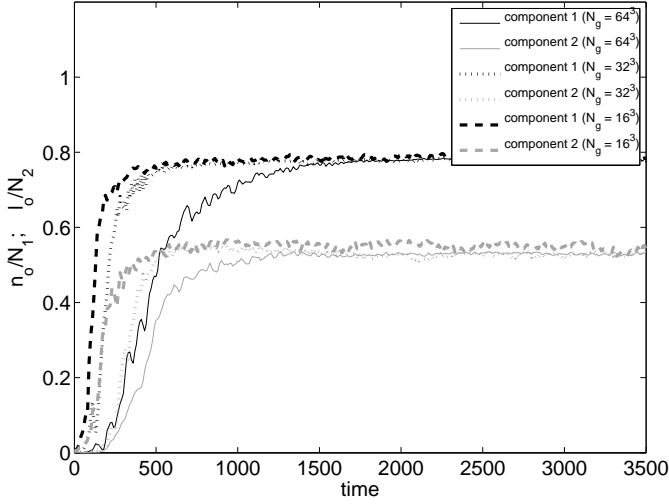


Fig. 1. Mass fractions as a function of time for three different grid sizes N_g . The other parameters were set to $H/V = 1.53$, $N_1/V = 0.5$, $N_2/V = 0.25$, $\alpha = 0.1$.

$$\begin{aligned} \langle H \rangle &= E_0 + \frac{(N_1 - n_o) \sum_k' \left(1 + \frac{k^2}{k^2 - \mu_2}\right)}{\sum_k' \frac{(k^2 + n_o/V)}{\omega_B^2(k)}}, \\ &= E_0 + \frac{N_2 \sum_k' \left(1 + \frac{k^2}{k^2 - \mu_2}\right)}{\sum_k' \frac{1}{k^2 - \mu_2}} \end{aligned} \quad (22)$$

and now

$$E_0 = \frac{1}{2V} [N_1^2 + (N_1 - n_o)^2 + 2N_2^2 + 2\alpha N_1 N_2]. \quad (23)$$

This equation provides two algebraic expressions for the two unknowns n_o and μ_2 . We note that at the critical energy where the condensate in the second component vanishes, we have $l_o = 0$ and $\mu_2 = 0$. At this point, it can be shown that the equilibrium distributions given by $\frac{T}{\Omega^+(k)}$ and $\frac{T}{\Omega^-(k)}$ reduce to $\frac{T}{\omega_B(k)}$ and $\frac{T}{k^2}$ and the two solutions given above match at the critical energy. This provides a solution for the thermodynamic state that is uniformly valid over the entire range of energies.

4. Numerical simulation

To verify the theory, we numerically solved the coupled system of equations (1) in a cubic region with periodic boundary conditions using a pseudo-spectral method. The initial conditions were set up using the random phase approximation (see e.g. [4]). To determine the properties of the system at equilibrium, we assumed that the ergodic hypothesis applies and used time-averages from our simulations to represent ensemble averages that arise in the theory presented above. We will firstly address the affect of the frequency cut-off on the thermodynamic equilibrium distributions predicted from our simulations. As explained above, the cut-off k_c is set by specifying the resolution in our computations. We have, therefore, performed simulations with

three different resolutions in a parameter regime where condensation occurs in both gases. Results for the evolution of the condensate mass fractions with time are shown in Fig. 1 for three different spatial resolutions. The results clearly reveal that the onset of the condensate formation (i.e. where Eq. (3) breaks down) and subsequent rate of growth, corresponding to the so called superfluid turbulence regime, are dependent on the grid resolution. This strong dependence of the turbulent state of the system on grid resolution is a well-known problem in non-dissipative classical systems. It typically arises from the bottleneck effect associated with energy spectrum pileup at high wave numbers [22]. However, as argued in Section 2, the final equilibrium mass fractions are independent of the resolution of the simulations. These results verify that, for the thermodynamic descriptions we wish to focus on in this work, introducing an ultraviolet cut-off does not affect the thermodynamic state. Given these observations, we will focus on the case with $N_g = 64^3$ in the remainder of this section.

The superfluid turbulence regime that leads to thermodynamic equilibrium can be visualised by tracking in time the evolution of the topological defects in the phase of the long wavelength part of the complex fields ψ_1 , and ψ_2 . Following the approaches used in [5], [16], we can accomplish this by filtering out the high frequency harmonics through the transformation $\hat{a}_{\mathbf{k}} \rightarrow a_{\mathbf{k}} \max\{1 - k^2/k_{cv}^2, 0\}$, $\hat{b}_{\mathbf{k}} \rightarrow b_{\mathbf{k}} \max\{1 - k^2/k_{cv}^2, 0\}$. k_{cv} is a cut-off wave number chosen according to the phenomenological formula $k_{cv} = 9 - t/1000$ in order to aid in the visualisation of the topological defects. Figure 2 shows the distribution of these defects at three different times. The density of the tangle clearly decreases with time as vortices annihilate that leads to a growing coherence length and hence condensate formation in analogy with the 2D results presented in [23]. The results described above correspond to a parameter range where both gases undergo condensation. If the initial total energy of the system is increased beyond some critical value, however, then we find condensation will occur in only one gas. This is clearly illustrated in Fig. 3 in terms of the contour plots of the topological defects of the two gases at different times for $H/V = 3.94$. To aid in the visualisation, we have produced separate plots of the tangle in each component. The plots clearly show the decreasing density of the defects with time in component one that is suggestive of the formation of a large coherent state. In contrast, no such ordering takes place in the second component which continues to exhibit many defects at later times. To further illustrate this behaviour at higher energies, we have included in Fig. 3 the growth of the condensate mass fractions at two different energies. The figure clearly shows that both gases undergo condensation when the initial total energy density $H/V = 1.53$, but only one gas condenses for an initial energy density of $H/V = 3.94$.

Having illustrated the formation of the condensates in our simulations, we will now compare the theoretical results derived in the previous section with predictions ob-

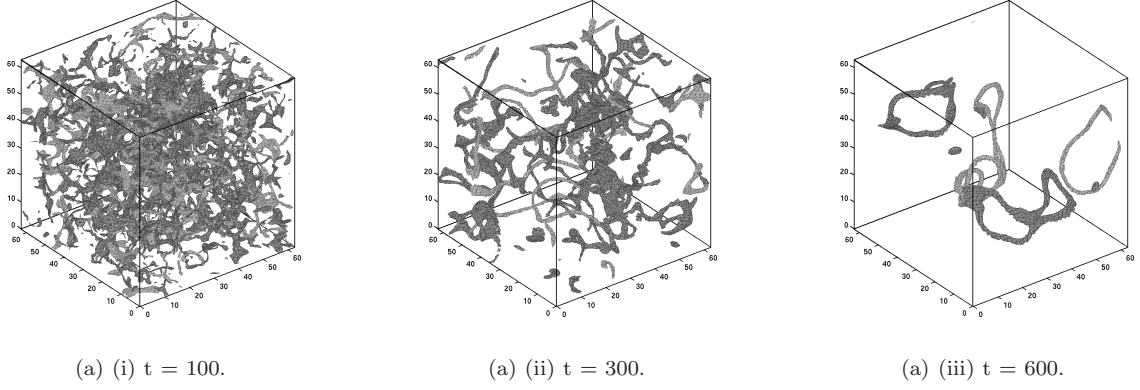


Fig. 2. Evolution of topological defects in the long wavelength parts of ψ_1 and ψ_2 denoted by $\hat{\psi}_1$ (light grey) and $\hat{\psi}_2$ (dark grey), respectively. The computational parameters are $H/V = 1.53$, $N_1/V = 0.5$, $N_2/V = 0.25$, $\alpha = 0.1$. The defects are visualised by iso-surfaces of $|\hat{\psi}_i|^2 = 0.04 \langle \hat{\psi}_i \rangle$ where $\langle \cdot \rangle$ is used here to denote a spatial average.

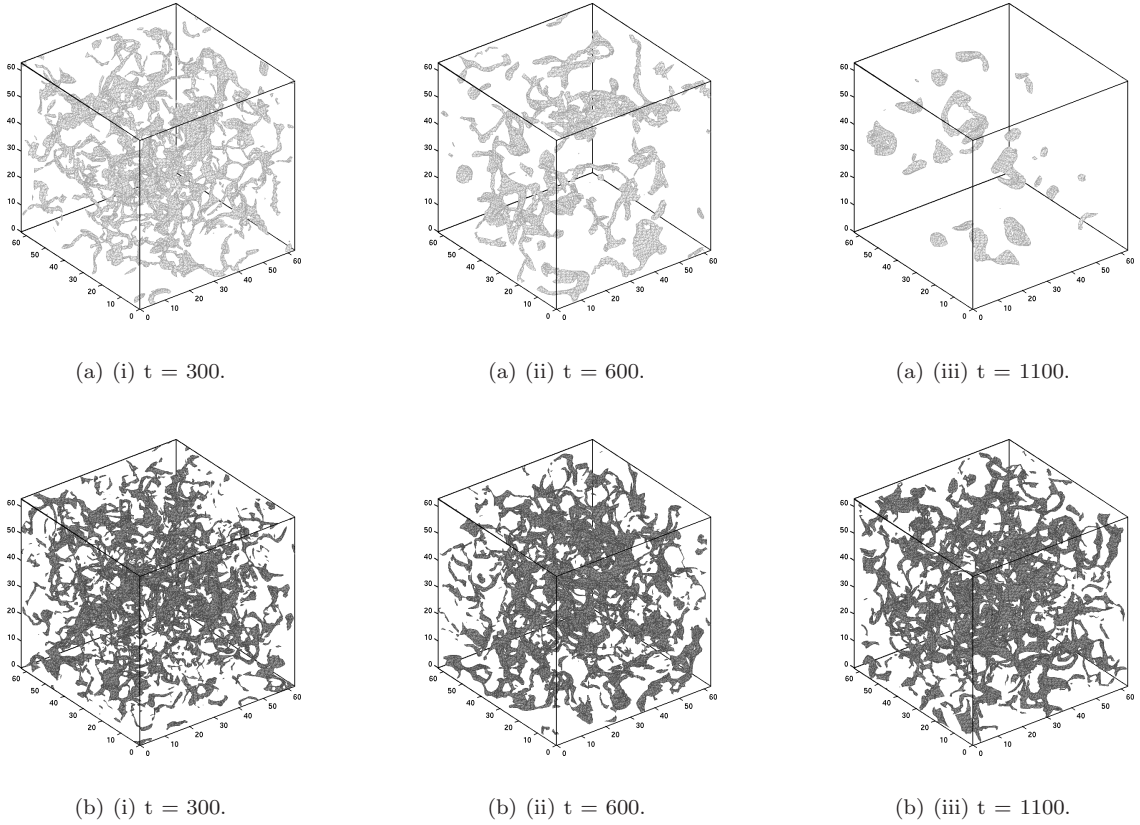


Fig. 3. Evolution of topological defects in the long wavelength parts of (a) ψ_1 and (b) ψ_2 denoted by $\hat{\psi}_1$ and $\hat{\psi}_2$, respectively. The computational parameters are $H/V = 1.53$, $N_1/V = 0.5$, $N_2/V = 0.25$, $\alpha = 0.1$. The defects are visualised by iso-surfaces of $|\hat{\psi}_i|^2 = 0.04 \langle \hat{\psi}_i \rangle$ where $\langle \cdot \rangle$ is used here to denote a spatial average.

tained from our computations. Figure 5 presents results for the variation of the condensate mass fractions with $\langle H \rangle / V$. The numerically computed condensate mass fractions were evaluated from a long time average once thermodynamic equilibrium was established. The results shown reveal remarkable agreement with the theory presented over the entire range of energies. For very large energies where only a small condensate mass fraction of the first component is

present, the theory deviates very slightly from the results of the simulations. This occurs since many particles are non-condensed in this region violating the assumption of a strong condensate that is required for the theory. Given the excellent agreement between the theory and predictions, we can use Eq. (22) to determine how the critical energy ($\langle H \rangle_{\text{crit}}$), at which condensation in the second component ceases, varies with the discrepancy parameter $\sigma = \frac{N_1 - N_2}{N_1}$.

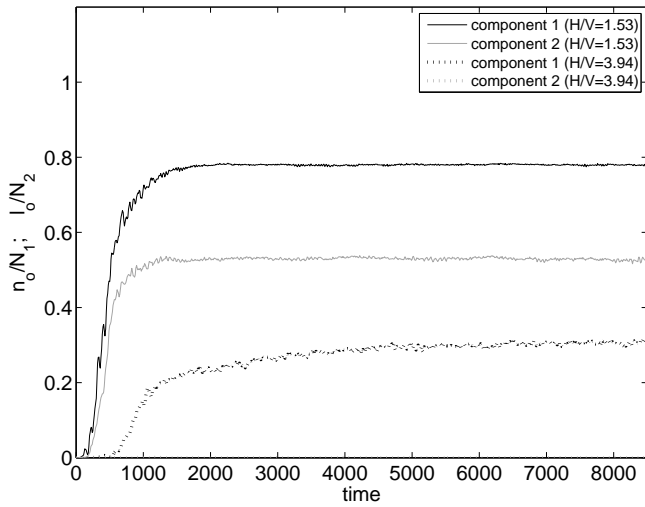


Fig. 4. Condensate mass fractions as a function of time for two different initial total energies. The systems' other parameters correspond to $N_1/V = 0.5$, $N_2/V = 0.25$, and $\alpha = 0.1$.

The variation of $\langle H \rangle_{\text{crit}}$, nondimensionalised with respect to the value at $\sigma = 0$ ($\langle H \rangle_{\text{ref}}$), is shown in the inset of Fig. 5. The figure clearly illustrates that $\langle H \rangle_{\text{crit}}$ deviates significantly from its value at $\sigma = 0$ as the discrepancy parameter is increased giving rise to a range of energies where only the first component condenses.

5. Conclusions

In this study we have derived a theoretical formulation of the thermodynamic state of a two-component Bose gas in the semi-classical approximation governed by the coupled NLS system of equations. The theory derived relies on the weak nonlinearity (small potential energies relative to kinetic energies) assumed for our system. The theory is based on a statistical formulation resulting in kinetic equations for the spectral number densities of each gas. Closure is achieved through the use of weak turbulence theory. Through detailed numerical simulations of the governing full dynamical equations, we have shown that the results are in excellent quantitative agreement with the theory. Moreover, we have illustrated that three parameters determine the final thermodynamic state of the system; the initial total energy H , and the total number of particles N_1 and N_2 in each gas. At very low energies, we have shown that condensation will occur in both gases whereas only one component condenses if the initial total energy is increased beyond some critical value that can be evaluated analytically.

The study presented here has focussed on the particular case of a two-component Bose gas mixture that exclude other forms of coupling (e.g. Josephson coupling). A natural next step will be to extend the theory to a more general class of two-component mixtures that include other types of interaction between the two components. Furthermore, the weak turbulence theory used in this work is applicable in the phase mixing regime. Indeed, the phase separation

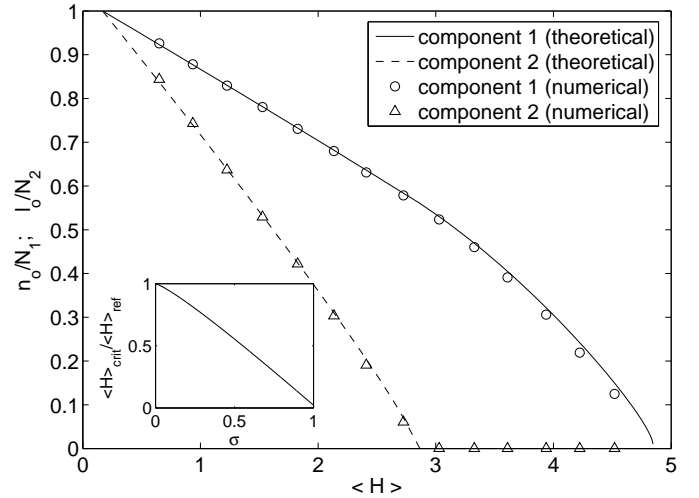


Fig. 5. Mass fractions as a function of averaged total energy for $N_1/V = 0.5$, $N_2/V = 0.25$, $\alpha = 0.1$; inset - non-dimensionalised critical energy as a function of discrepancy parameter.

regime, which has not been considered in this work, exhibits a rich class of behaviour that can not be analysed using the approaches described in this work. An in-depth study of the condensation in this regime remains an essential step for a complete understanding of condensation in systems composed of Bose gas mixtures.

We end by noting that given the universality of the coupled NLS system of equations, the study presented here is relevant in quantifying condensation in a number of physical systems. In addition to the Bose gas mixtures at finite temperature considered in this work, the results are equally relevant to the field of nonlinear optics provided many modes are present that can be modeled semi-classically (see e.g. [24] for an analogous study of the one component system).

Acknowledgments

The authors acknowledge support from EPSRC-UK under Grant No. EP/D032407/1 and Boris Svistunov for many useful discussions.

References

- [1] V.E. Zakharov, A.N. Pushkarev, V.F. Shvets, and V.V. Yan'kov, *JETP Lett.* **48**, 83 (1988); S. Dyachenko, V.E. Zakharov, A.N. Pushkarev, V.F. Shvets, and V.V. Yan'kov, *Sov. Phys. JETP*, **69**, 1144 (1989).
- [2] V.L. Ginzburg and L.P. Pitaevskii, *Sov. Phys. JETP*, **7**, 858 (1958); L.P. Pitaevskii, *Sov. Phys. JETP*, **13**, 451 (1961); E.P. Gross, *J. Math. Phys.* **4**, 195 (1963).
- [3] B.V. Svistunov, *J. Moscow Phys. Soc.* **1**, 373 (1991); Yu. Kagan, B.V. Svistunov, and G.V. Shlyapnikov, *Zh. Eksp. Teor. Fiz.* **101**, 528 (1992) [*Sov. Phys. JETP* **75**, 387 (1992)]; Yu. Kagan and B.V. Svistunov, *Zh. Eksp. Teor. Fiz.* **105**, 353 (1994) [*Sov. Phys. JETP* **78**, 187 (1994)]; Yu. Kagan and B.V. Svistunov, *Phys. Rev. Lett.* **79**, 3331 (1997).

- [4] M.J. Davis, S.A. Morgan, and K. Burnett, *Phys. Rev. Lett* **87**, 160402 (2001); *Phys. Rev. A* **66**, 053618 (2002).
- [5] N.G. Berloff and B.V. Svistunov, *Phys. Rev. A*, **66**, 013603 (2002).
- [6] C.J. Myatt, E.A. Burt, R.W. Ghrist, E.A. Cornell, and C.E. Wieman, *Phys. Rev. Lett.* **78**, 586 (1997); D.S. Hall, M.R. Matthews, J.R. Ensher, C.E. Wieman, and E.A. Cornell *Phys. Rev. Lett.* **81**, 1539 (1998); D.M. Stamper-Kurn, M.R. Andrews, A.P. Chikkatur, S. Inouye, H.-J. Miesner, J. Stenger, and W. Ketterle *Phys. Rev. Lett.* **80**, 2027 (1998); and J. Stenger, S. Inouye, D.M. Stamper-Kurn, H.-J. Miesner, A.P. Chikkatur, and W. Ketterle, *Nature*, **396**, 345 (1998).
- [7] G. Modugno, M. Modugno, F. Riboli, G. Roati, and M. Inguscio, *Phys. Rev. Lett.* **89**, 190404 (2002).
- [8] N.G. Berloff and A.J. Youd, *Phys. Rev. Lett.* **99**, 145301 (2007).
- [9] T.W.B. Kibble, *J. Phys. A* **9**, 1387 (1976) and W.H. Zurek, *Nature* **317**, 505 (1985).
- [10] N.G. Berloff, *Phys. Rev. Lett.* **94**, 010403 (2005).
- [11] see e.g. S.V. Manakov, *Sov. Phys. JETP*, **38**, 248 (1974); G.P. Agrawal, P.L. Baldeck, and R.R. Alfano *Phys. Rev. A*, **39**, 3406 (1989).
- [12] C. Connaughton, C. Josserand, A. Picozzi, Y. Pomeau, and S. Rica *Phys. Rev. Lett.* **95**, 263901 (2005).
- [13] H. Shi, W.-M. Zheng, and S.-T. Chui, *Phys. Rev. A*, **61**, 063613 (2000); E. Timmermans, *Phys. Rev. Lett.* **81**, 5718 (1998).
- [14] V.E. Zakharov, V.S. L'vov and G. Falkovich, *Kolmogorov Spectra of Turbulence I* (Springer, Berlin, 1992); A.C. Newell, S. Nazarenko, L. Biven, *Physica D*, **152**, 520 (2001).
- [15] M.J. Davis, R.J. Ballagh, and K. Burnett *J. Phys. B: At. Mol. Opt. Phys.*, **34**, 4487 (2001); M. Brewczyk, M. Gajda, and K. Rzażewski *J. Phys. B: At. Mol. Opt. Phys.* **40**, R1-R37 (2007).
- [16] N.G. Berloff and C. Yin, *J. Low Temp. Phys.* **145**, 187 (2006).
- [17] N.N. Bogoliubov, *J. Phys.* **11**, 23 (1947).
- [18] P. Tommasini, E.J.V. de Passos, A.F.R. de Toledo Piza, M.S. Hussein, and E. Timmermans *Phys. Rev. A*, **67**, 023606 (2003); see also W.B. Colson and A.L. Fetter, *J. Low Temp. Phys.* **33**, 231 (1978).
- [19] R. Lacaze, P. Lallemand, Y. Pomeau, and S. Rica, *Physica D*, **152**, 779 (2001).
- [20] C. Connaughton, and Y. Pomeau, *C.R. Physique* **5**, 91 (2004).
- [21] S. Dyachenko, A.C. Newell, A. Pushkarev, and V.E. Zakharov, *Physica D*, **57**, 96 (1992).
- [22] G. Falkovich, *Phys. Fluids* **6**, 1411 (1994).
- [23] S. Nazarenko, and M. Onorato, *J. Low Temp. Phys.* **146**, 31 (2007).
- [24] A. Picozzi, *Optics Express*, **15**, 9063 (2007).